EVS 30 Symposium
Stuttgart, Germany, October 9 – 11, 2017

48 V – the Future of Automotive Traction

Florian Bachheibl[1], Adrian Patzak[1], Martin Ehmann[2], Benjamin Rubey[1], Oleg Moros[1], Dieter Gerling[3]

[1] volabo GmbH, Alte Landstraße 23 – 85521 Ottobrunn, florian.bachheibl@volabo.com
[2] TESIS DYNAware GmbH
[3] Universitaet der Bundeswehr Muenchen

Summary

A new approach to automotive traction motors - the Intelligent Stator Cage Drive (ISCAD) - is presented on the component level and on full vehicle system level. A comparison between a conventional BEV and a vehicle equipped with the new drive is carried out with respect to driving cycle efficiency. ISCAD outperforms a PM- and IM-based drive by 15 to 25 % in driving cycle energy consumption.

Keywords: electric drive, BEV, high efficiency, asynchronous (induction) motor, high safety

1. Introduction

Most electric vehicles of the current generation feature battery voltages of between 300 and 500 VDC, whilst there seems to be a tendency for an even further increase towards 800 VDC. The major argument for this doubling is the simultaneous doubling of fast charging power if a hand-pluggable power connection is chosen. Drives operating at this voltage are typically controlled via IGBT-based inverters, since SiC-based power electronics are still too expensive for a mass application. They usually exhibit wound or welded copper coils to form the magnetic field inside the motor. Both technology choices are far from optimal as will be shown in the following section. After introducing the low voltage high power **I**ntelligent **S**tator **Ca**ge **D**rive (ISCAD), its advantages and challenges will be discussed before a car topology is presented.

2. The ISCAD Principle

2.1. The Electric Motor

In conventional electric machines, enameled copper windings are used to form the link between electrical and magnetic domain. They don't constitute an optimal technical solution for three main reasons:

- In mass manufacturing, slot fill factors above 40 % are hard to reach, causing a high electrical resistance and a poor thermal path to the stator iron
- To keep electrical resistances as low as possible, expensive copper has to be chosen as conductor
- The layered insulation system is complex, costly to produce and very fragile which accompanies high scrap rates.

For these reasons, much effort has been invested into the improvement of the winding system, which led to concentrated and hairpin-windings. Nevertheless, the problems mentioned above have only been mitigated, but not solved.

ISCAD proposes a radical approach to the mentioned problems by replacing the winding with a stator cage, which is similar to an induction motor's squirrel cage with one short circuit ring removed. Accounting for a thin layer of slot insulation, this method allows for fill factors above 90 %, thus giving way for a widespread use of aluminum as conductor material, see Fig. 1a). In addition, this stator cage can be mass-manufactured easily and in a very stable process by various well-established production technologies. Finally, the stator cage is thermally more rugged than an enamel-coated copper conductor. This, in combination with the low phase voltage, allows ISCAD to tap in to the large overload area marked in the figure. Full torque can be achieved far above base speed for a short period of time.

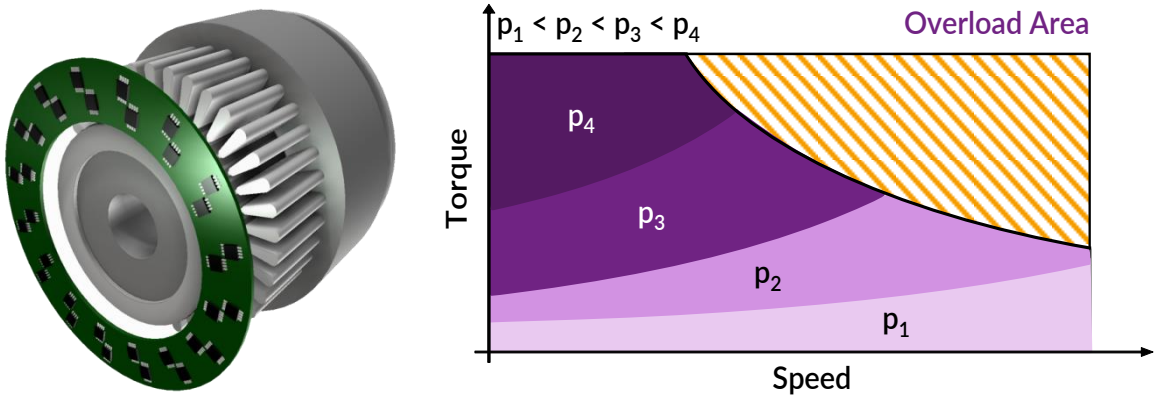

Figure 1: a) Stator Cage Drive b) Principle of load-dependent pole pair selection

Aside from the advantages in manufacturing, the stator cage motor allows for a smoother airgap MMF, since the current loading of every slot can be controlled individually and not only in multiples of the conductor current. This effect increases the winding factor of the operating wave by 4 % and reduces the THD in the same way, thus reducing losses both in stator and rotor [1]. What is more, the amount of pole pairs that are created by the stator cage can be changed without any changes in torque if it is combined with an induction rotor. This feature gives rise to another degree of freedom in machine control. Whilst conventional machines have a fixed number of pole pairs, thus having only one region of optimum efficiency, the stator cage machine can add up regions of optimum efficiency for several numbers of pole pairs, which greatly increases the overall region of best efficiency, see Fig. 1b).

2.2. The Inverter

As the stator-cage winding only forms one turn, the induced voltages are very low. It is therefore possible to not only use MOSFET-switches, but even to stay within the safe-to-touch voltage range below 60 VDC and 30 VAC. Apart from the large gain in intrinsic safety, devices with higher doping and therefore lower

resistance can be used if compared to high voltage devices. If the high-voltage inverter is IGBT-based, its devices feature a diode-like loss characteristic, which translates to a poor partial-load-efficiency, see Figure 2. Moving from an IGBT-based drive to one that is MOSFET-based contributes to a large gain in partial-load efficiency.

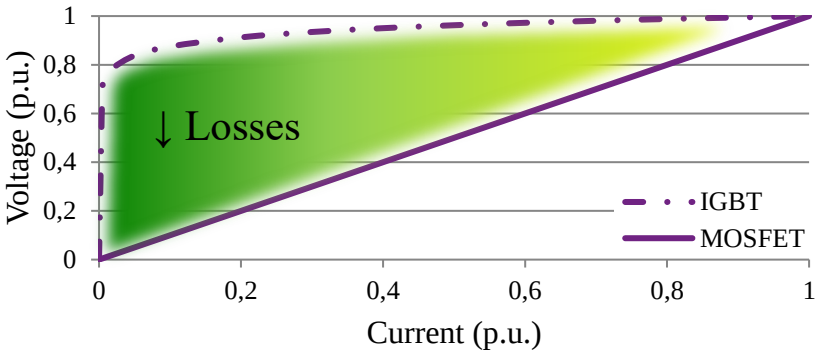

Figure 2: Forward voltage drop of IGBT and MOSFET versus forward current

2.3. The DC Supply System

One of the most often seen objections to BEV traction motors operating with 48 V is the size of the supply system. It is at first counter-intuitive that it is easily possible to transfer as much as 3 kA in a vehicle supply system. However, it is a big difference if continuous power is to be transmitted over several hundred kilometers from power plants to users or if power is transmitted over short distances in a highly dynamical way. The rated power of an electric luxury sedan on the market, for example, is only 70 kW. Transmitting this power in a 48 V automotive supply system is not at all challenging – although currently not well-known to the industry. An aluminum conductor of 400 mm² could transport this power continuously, while allowing for multiples of this value as peak loads. This is smaller than the smallest surface of a match box. In total, less than 5 kg of material with a cost of less than 5 € has to be used for both poles if transmission of a peak power up to 200 kW over a distance of 1.5 m is considered.

3. Driving Cycle Analysis

The advantages of motor and inverter combined yield an increase in driving cycle efficiency of 20 to 25 % in the WLTC [2] if compared to an otherwise identical high voltage alternative that is based on an induction machine. This allows for a significant reduction of battery size for a given driving range, or for an increased driving range with the identical battery capacity. The comparison in [2] was based on a high-power sedan with over 600 Nm of torque and an induction machine. In part of the academic and automotive community, this raised the objection of being an unfair comparison. On the one hand, applying typical driving cycles to such a powerful drivetrain means a very low load beneath 30 % of the maximum torque. On the other hand, an induction machine was considered far inferior to PM machines when it comes to overall efficiency. It is this paper's aim to prove that ISCAD is also advantageous in lower powered vehicles, even if they are equipped with a PM machine. The comparison with a conventional induction machine is added for the sake of completeness.

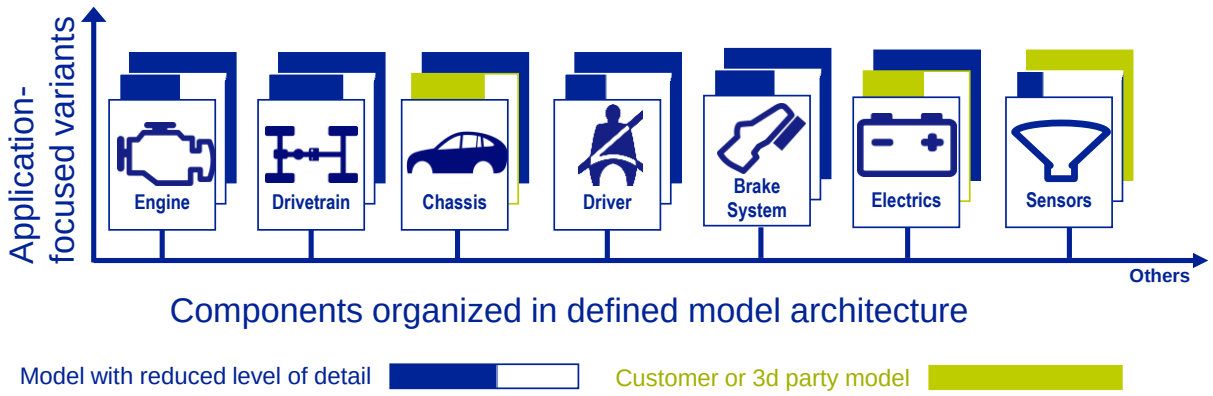

Figure 3: Model repository with components of different level of fidelity in DYNA4

3.1. Simulation Environment and Vehicle/Drivetrain Model

For evaluation of the drives' performance in a vehicle, the vehicle system simulation package DYNA4 Advanced Powertrain by TESIS DYNAware is used. This package comprises of a 1D drivetrain model, dual-voltage supply system, vehicle, brake-system, road and driver models. In the DYNA4 [3] packages, every vehicle component is available in different level of model fidelity or different model type. For all components, the appropriate level of model fidelity may be chosen for different simulation applications – from very fast running models for energetic analysis to HIL tests of vehicle dynamics or drivetrain control ECUs [4], [5], see Figure 3.

Thanks to the modular model architecture implemented in Simulink, especially the drivetrain and supply system models may be combined with any vehicle model – starting from a purely longitudinal roller dynamometer model, thereafter a single-track model, up to full 3D vehicle dynamics and tire model.

DYNA4 Advanced Powertrain is well suited for detailed analysis of the energy flow from battery to wheel in a BEV. It comprises of a replacement circuit model for the batteries, where 12 V and 48 V batteries were used here, as well as a supply system, including cable losses and different types of electric consumers, such as ohmic or constant power consumers, see Figure 4. Efficiency map based models were used for inverters and for PM, induction and ISCAD motors.

Efficiency maps for transmission and differential are based on rotational speed, transmitted torque and component lubricant temperature. The temperature dependency was, however, neglected in the current investigation since temperature based measurements of the mechanical components were not available. The drivetrain components, such as mechanical parts of motor, transmission and differential were modeled as ideal rotational inertias (1D) and interconnected by rigid shafts. For more detailed drivetrain analysis, elastic shafts and other force elements such as clutches and torque vectoring differentials, are also available in DYNA4.

For the energetic analysis of the simulation results, DYNA4 Advanced Powertrain provides a visualization of all energy flows in each simulation step, e.g. input and output power of all electric and mechanical modules. Also, a summary of the total input, output and dissipated (thermal) energy of all components for drive and recuperation mode is automatically generated as an Excel sheet at the end of a simulation run. The used driving cycles are readily available as simulation tasks in the tool.

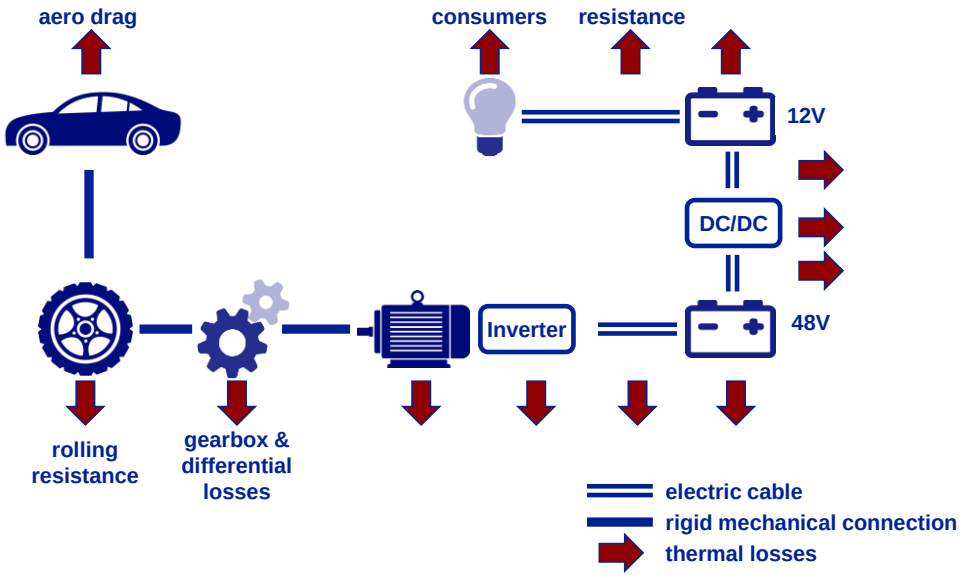

Figure 4: Basic structure of the DYNA4 model for energy analysis

3.2. Vehicle Parameters

The vehicle chosen for the analyses is a mass-market model of a Chinese car manufacturer. It is available in several configurations, namely an ICE configuration and a pure BEV configuration. The BEV model uses a permanent magnet machine that delivers 42 kW continuously and 106 kW of peak performance. The vehicle's electric drive features an overload torque of 240 Nm until a base speed of 4200 rpm. Apart from the outer size, no further data of the motor was available. All three considered drives were designed by the authors as laid out in the next section. Further data used to parameterize the vehicle model are listed in Table 1. How the efficiency maps of inverter and motor were obtained is described in the following two sections.

Table 1: Vehicle parameters for the investigated platform

Parameters	Value
Air drag coefficient	0.29
Front surface	2.2 m²
Tire radius, unloaded	0.32 m
Rolling resistance coefficient	0.014
Vehicle mass	1600 kg
Transmission ratio shaft to wheel	7.2
Transmission efficiency	0.96

3.3. Generation of the electric motor efficiency maps

The electric motors were designed to meet the requirements defined in 3.2 and their efficiency maps were generated using ANSYS Maxwell. For the PM machine, an automated tool was used to find the optimal load angle for each torque-speed-point. For the ISCAD machine and the IM machine, which are both equipped with a squirrel cage rotor, an own script has been used to obtain the optimal slip under the boundary conditions of maximum current and voltage. PM eddy current loss and eddy current, resp. skin effect loss was considered for both ISCAD and the IM in the stator and rotor cages. Aside from the efficiency data points, the machine simulation also yielded values for the power factor, current, voltage and frequency to be used for power electronics design and loss estimation. An overview of relevant data is given in Table 2.

Table 2: Relevant data for the considered machines

	PM	ISCAD	IM
Stack diameter	230 mm	230 mm	230 mm
Stack length	137 mm	185 mm	190 mm
Maximum RMS phase current	300 A	600 A	350 A
Maximum RMS phase voltage	137 V	13 V	137 V
Number of phases	3	42	3
Mass (active parts)	38 kg	45 kg	52 kg
Material Costs (active parts)	100 %	25 %	35 %

3.4. Generation of the power electronics efficiency maps

Two inverter configurations have been designed – a three-phase IGBT-based inverter for the HV induction and permanent magnet machines and a multi-phase MOSFET-based inverter for ISCAD. In order to generate the power electronics efficiency map, the values that resulted from the machine analysis were used to analytically calculate the losses. All relevant loss components were considered, including the power electronics switches, the bus bars and the capacitors. This loss component is especially relevant for ISCAD with its higher phase currents [6], [7]. The parameters for the power loss calculations are listed in Table 3 for the IGBT-based and MOSFET-based inverters. The MOSFET-based inverter is an in-house design and well known, whereas the parameters of the IGBT-based inverter were adapted to the presented application out of a referred third-party design. The equations for the calculation of the power losses of the semiconductors were derived from [8] [9].

Table 3: Parameters of IGBT-based and MOSFET-based inverters for power loss calculations

	IGBT-based	MOSFET-based
U_{DC}	400 V	48 V
f_{switch}	12 kHz	25 kHz
U_{Driver}	15 V	15 V
$U_{Plateau}$	-	4.4 V
t_{ri}	-	80 ns
t_{fi}	-	80 ns
R_{Gate}	-	5.2 Ω
Q_{rr}	8.5 µQ	318 nQ
C_{GD1}	-	60 pF
C_{GD2}	-	2.7 nF
$T_{Junction}$	95°C	95°C
$R_{DSon(95°C)}$	-	1.4 mΩ
$n_{Switches\_parallel}$	6	4
$ESR_{Capacitors}$	0.4 mΩ	0.13 mΩ
R_{Cable}	76 µΩ	25.7 µΩ
$R_{Connectors}$	80 µΩ	50 µΩ
u_{CE0}	1.4 V	-
r_C	4 mΩ	-
U_{D0}	1.3 V	-
r_D	5.4 mΩ	-
E_{on}	3.5 mJ	-
E_{off}	1.5 mJ	-

3.5. Selected Driving Cycles

As already stated in the introduction to this section, a high emphasis shall be put on selecting driving cycles which represent real driving. According to [10], the acceleration time from 0 to 100 km/h in real driving has decreased from 14 to 9 seconds between 1981 and 2007. Even though the NEDC was updated for highway driving in 1990 [11] by adding the “Extra-Urban Cycle”, it doesn’t account for this increased acceleration. Figure 5 shows the torque-speed-locus of the NEDC. In addition, it displays the dwell time in certain torque-speed regions by colored rectangles. The iso-efficiency lines drawn in the figure represent the efficiency of ISCAD. Since the drive is designed to deliver a peak torque of 240 Nm, only 50 % of the maximum torque is requested in the NEDC. The same holds true for the power. The maximum power in motor mode is 38 kW and 40 kW in generator mode, although the drive has a peak power of 110 kW.

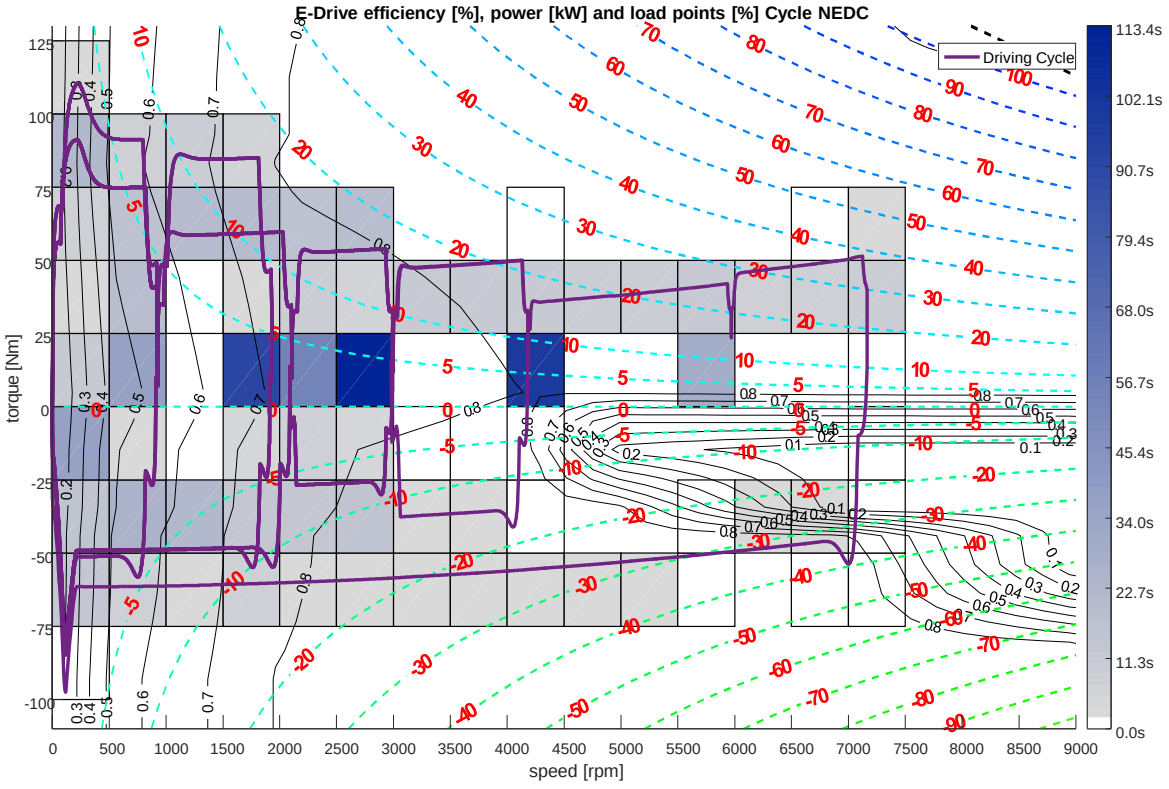

Figure 5: Power, loadpoints and ISCAD Drivetrain efficiency in the NEDC

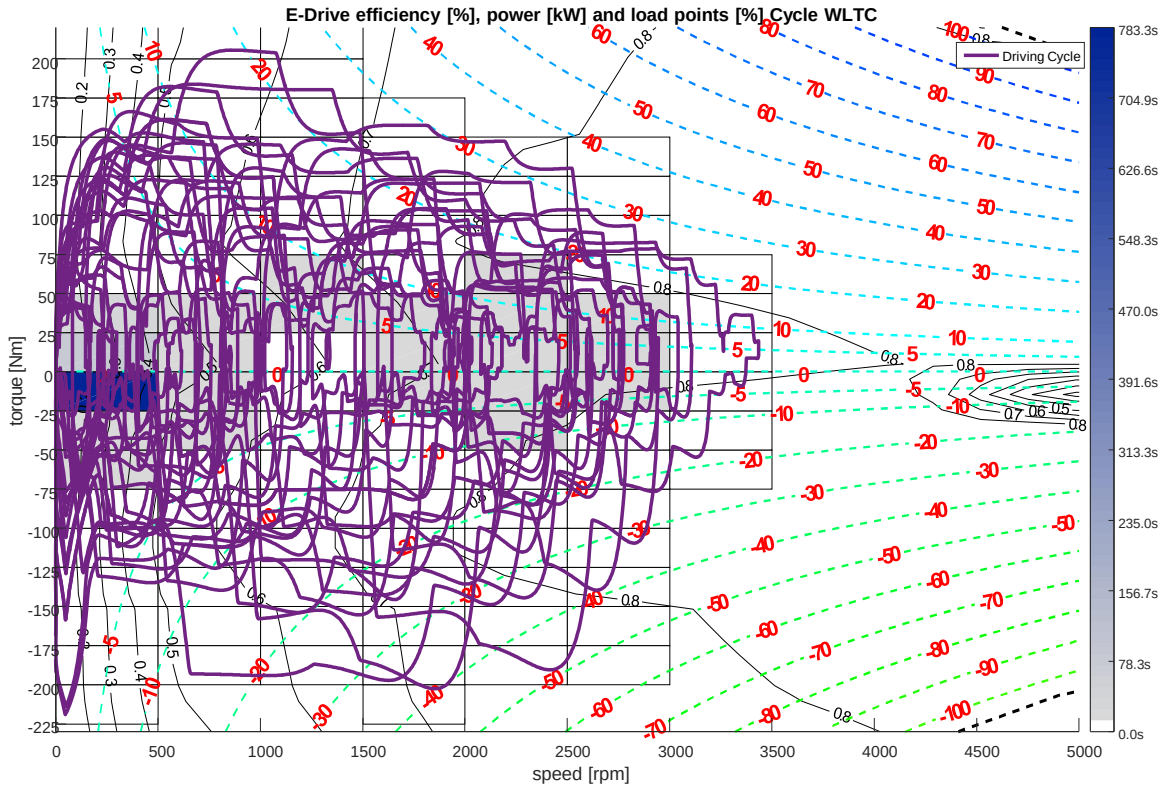

Figure 6: Power, loadpoints and ISCAD Drivetrain efficiency in the WLTC

The lack of realism in the NEDC has been acknowledged by the authorities and it will therefore be replaced by the WLTC once all relevant regulations are passed. Figure 6 shows the torque-speed locus of the WLTC, including the dwell times for the applicable torque-speed regions and the iso-efficiency lines for ISCAD. Obviously, this cycle demands a lot more torque and also a fraction more power than the NEDC.

In addition to the two cycles mentioned above, the CADC Urban (Artemis Urban Cycle) cycle has been chosen. It was generated with reference to real driving accelerations and requires similar torques to the WLTC.

Comparing the three drive cycles, different drivetrain efficiencies may be expected due to the differing load points and respective dwell times. Also, the energy dissipated in the vehicle depends strongly on the drive cycle. Since both WLTC and NEDC feature a highway period, air drag plays a more dominant role than in the Artemis Urban cycle. This also reflects in the percentage of recoverable energy in Table 4. The table shows both the energy flow from the wheel's perspective and from the perspective of the motor shaft. In the first case, only air drag, tire friction and kinetic energy are considered. In the latter case, the energy lost by the transmission and the differential is also included. Part of the difference results from the different cycle profiles and part of it arises from the different cycle lengths. The NEDC covers a distance of 11 km, the WLTC is 23.3 km long and the Artemis Urban cycle has a length of 4.5 km.

Table 4: Dissipated energy in the considered cycles, using wheel and shaft as perspectives

	NEDC	WLTC	Artemis Urban
Energy Applied, Wheel [Wh]	1481	3525	879.4
Energy Recuperated, Wheel [Wh]	407.8	855.8	529.4
Energy Balance, Wheel [Wh]	**1073.2**	**2669.2**	**350**
Energy Applied, Motor Shaft [Wh]	1547	3681	920.9
Energy Recuperated, Motor Shaft [Wh]	396.2	833.5	513.8
Energy Balance, Motor Shaft [Wh]	**1150.8**	**2847.5**	**407.1**

3.6. Results

Table 5 lists the applied and recuperated energy and the energy balance or used energy for the considered cycles and for all considered drivetrains. Figure 7 displays the results in graphical form.

Table 5: Energy usage, recuperation and balance in the selected cycles

	NEDC	WLTC	Artemis Urban
Energy Applied, PM [Wh]	2563	5531	1503
Energy Recuperated, PM [Wh]	252.8	564.9	355.9
Energy Balance, PM [Wh]	**2310.2**	**4966.1**	**1147.1**
Energy Applied, IM [Wh]	2607	5580	1607
Energy Recuperated, IM [Wh]	247.9	550	335.8
Energy Balance, IM [Wh]	**2359.1**	**5030**	**1271.2**
Energy Applied, ISCAD [Wh]	2035	4655	1353
Energy Recuperated, ISCAD [Wh]	307.3	660	379
Energy Balance, ISCAD [Wh]	**1727.7**	**3995**	**974**

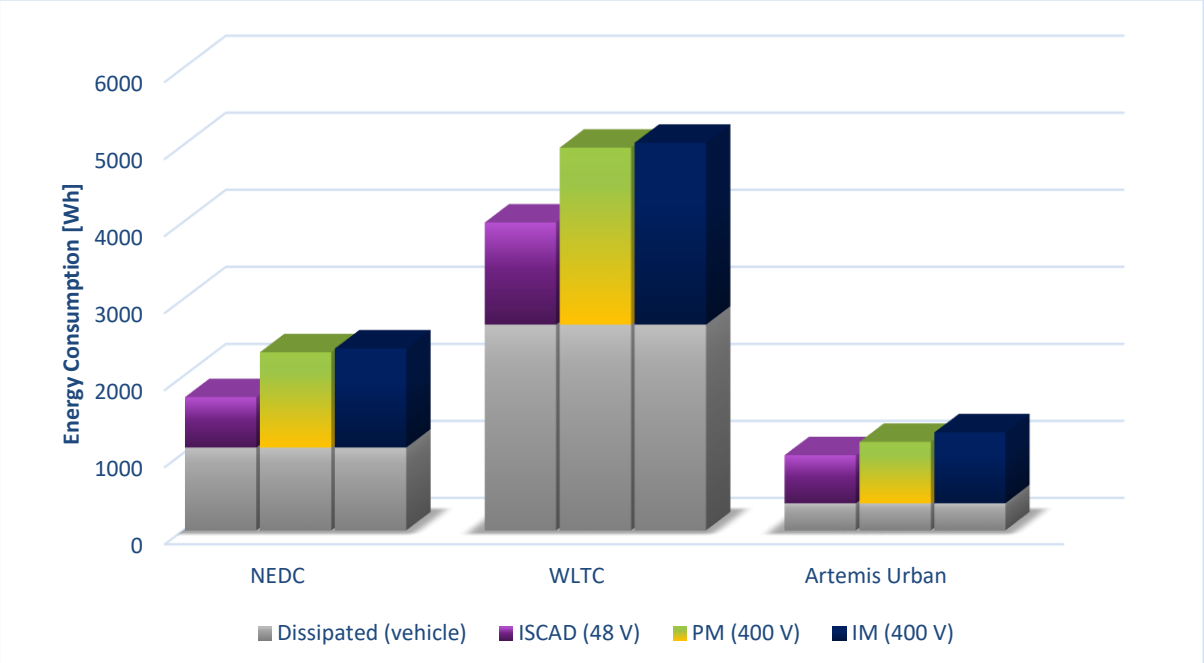

Figure 7: Visualization of the cycle energy usage

Figure 7 shows the energy dissipated by the vehicle and mechanical drivetrain (grey), the energy dissipated by ISCAD (inverter and motor, purple), the energy dissipated by PM and induction motor drive (orange/green and dark blue). Thus, the total energy consumption of ISCAD is “grey + purple”, for the PM it is “grey + + orange/green” and the total for the induction motor is “grey + dark blue”.

The dissipated energies are higher than the manufacturer’s declaration of 17,6 kWh/100 km. Measurements on a test track in real driving situations however indicate a consumption of as much as 22 kWh/100 km, which is in very good agreement with the simulated consumption in the WLTC and Artemis Urban cycle. The reduction in energy consumption varies between 15% (CADC Urban) and 25 % (NEDC) when exchanging the PM drive with ISCAD. The advantage against an induction machine is even higher.

4. Conclusion and Outlook

Three drives have been designed for a given vehicle to match the type plate of the vehicle’s PM machine. The electric machines have been simulated in FEA using ANSYS Maxwell and the inverters were simulated using an analytic tool. The resulting efficiency maps for both motor and generator mode were applied to the comprehensive vehicle simulation framework DYNA4 by TESIS DYNAware in order to perform driving cycle analyses of energy consumption. The NEDC, WLTC and CADC Urban cycles have been chosen for reference. In all three cycles, a clear advantage for ISCAD could be obtained. It consumes between 15 and 25 % less energy than the other two conventional high-voltage drives. Being able to convert traction power with higher efficiency means a huge advantage to the state-of-the-art. Either, the battery can be reduced by a bit more than 15 to 25 % for equal range (reduced battery weight means even less energy consumption). Or, the achievable range can be increased by the numbers above.

Above all, the drive operates at a voltage of 48 V. This means intrinsic electrical safety for drivers, passengers, for the manufacturers and in maintenance. Cost reductions can be achieved by economizing on the otherwise required HV protection. In addition, power electronic components are cheaper for low voltage which overcompensates the required number of switches in a multi-phase drivetrain.

The drive is currently being tested on a test bench in the exact setup that has been published in this document. After extensive measurements, it will be built into a vehicle for road testing. Further publications on the measurement- and road-test-results are intended in the near future.

References

[1] G. Dajaku and D. Gerling, "Low costs and high efficiency asynchronous machine with stator cage winding," in *2014 IEEE International Electric Vehicle Conference (IEVC)*, Florence, 2014.

[2] A. Patzak, F. Bachheibl, A. Baumgardt, G. Dajaku, O. Moros and D. Gerling, "Driving range evaluation of a multi-phase drive for low voltage high power electric vehicles," in *2015 International Conference on Sustainabe Mobility Applications, Renewables and Technology (SMART)*, Kuwait City, 2015.

[3] O. Philipp, M. Ehmann, T. Butz and S. Diel, "Effizienter Einsatz von Fahrzeug-Funktionsmodellen in der Komponenten- und Regelsystemenwicklung," in *Simulation und Test*, Berlin, 2010.

[4] M. Vockenhuber, M. Ehmann and T. Ruckenbauer, "Funktionsapplikation für Allrad-Traktionsregelsysteme. Ein Expertentool für die klassische und modellbasierte Applikation verschiedener 4WD Traktionssystem-Architekturen.," in *1. Automobiltechnisches Kolloquium*, München, 2009.

[5] A. Pinnel, T. Butz, M. Ehmann and H. Fan, "Vehicle Dynamics Simulation with Active Yaw Control using Variable Drive Torque Distribution," in *Society of Automotive Engineers of Japan, JSAE Paper 20045411*, Yokohama, 2004.

[6] B. Rubey and D. Gerling, "Design of high current low voltage half-bridges for multi-phase inverter application in the ISCAD drive," in *2016 19th International Conference on Electrical Machines and Systems (ICEMS)*, Chiba, 2016.

[7] B. Rubey, A. Patzak, F. Bachheibl and D. Gerling, "DC-Link Current Harmonics Minimization in ISCAD Multi-Phase Inverters with Interleaving," in *IEEE-VPPC Vehicle Power and Propulsion Conference*, Belfort, France, 2017 [to be published].

[8] D. Graovac, M. Pürschel and A. Kiep, "IGBT Power Losses Calculation Using the Data-Sheet Parameters," Infineon Application Note, Neubiberg, 2009.

[9] D. Graovac, M. Pürschel and A. Kiep, "MOSFET Power Losses Calculation Using the Data-Sheet Parameters," Infineon Application Note, Neubiberg, 2006.

[10] S. E. Plotkin, "Examining Fuel Economy and Carbon Standards for Light Vehicles. Discussion Paper No. 2007-1," OECD-ITF Joint Transport Research Centre, OECD Publishing, Paris, 2007.

[11] *"Agreement concerning the adoption of uniform technical prescriptions for wheeled vehicles [...] and the conditions for reciprocal recognition of approvals granted on the basis of these prescriptions.*, E/ECE/TRANS/505/Rev.2/Add.100/Rev.3, E/ECE/324/Rev.2/Add.100/Rev.3 or, 2013.

Authors

Florian Bachheibl, M.Sc. (volabo GmbH – Alte Landstraße 23, 85521 Ottobrunn, Germany – Email: florian.bachheibl@volabo.com – Url: www.volabo.com) Born in 1987, he graduated from the Universitaet der Bundeswehr Muenchen in 2011 with a Master of Science in mechatronics engineering. He then joined the Institute of Electrical Drives and Actuators as a research assistant where he conducted research in the areas of modelling of passive components, systems engineering and fields analysis before he switched to volabo GmbH as a co-founder and managing director in 2016.

Adrian Patzak, M.Sc (volabo GmbH – Alte Landstraße 23, 85521 Ottobrunn, Germany – Email: adrian.patzak@volabo.com – url: www.volabo.com) Adrian Patzak was born in 1985 and received his Master degree in Electrical Engineering from the University of Applied Sciences Regensburg, Germany, in 2011. Afterwards he joined the University of Federal Defense Munich, and was working as a research assistant on Automotive Power Systems, Electric Machines and Control before he switched to volabo GmbH as a co-founder and managing director in 2016.

Martin Ehmann, Dipl. Math. Univ. (TESIS DYNAware GmbH – Baierbrunner Straße 15, 81379 Munich, Germany – Email: martin.ehmann@tesis.de – url: www.tesis-dynaware.com) Martin Ehmann, born in 1970, got his diploma in Mathematics from Technical University of Munich in 1997. His diploma thesis on vehicle simulation, was awarded a prize by the Association of German Engineers (VDI). After working for two federal German research projects on driver modeling in cooperation with TESIS, he joined TESIS DYNAware in 2001 as a developer for vehicle dynamics. Since then, he held several positions in product development, product management and as senior consultant.

Benjamin Rubey (volabo GmbH – Alte Landstraße 23, 85521 Ottobrunn, Germany – Email: benjamin.rubey@volabo.com – url: www.volabo.com) Benjamin Rubey was born in 1987 in Munich, Germany. He obtained his M.Sc. degree in Electrical Engineering from the Technical University of Munich (TUM) in 2012. Between 2013 and 2015 he had worked at GIGATRONIK GmbH and was responsible for securing the electrical drivetrain of plug-in hybrid cars. Afterwards he switched to FEAAM GmbH as a research assistant in cooperation with the Institute of Electrical Drives and Actuators for the development of low-voltage inverter topologies in 2015. His current position is developer of power electronics at volabo GmbH since 2016.

Oleg Moros, M.Sc. (volabo GmbH – Alte Landstraße 23, 85521 Ottobrunn, Germany – Email: oleg.moros@volabo.com – url: www.volabo.com) Born in 1984, he graduated from the University of Federal Defense Munich in 2011 with a Master of Science in mathematical engineering. He then joined the Research Center for Electrical Drives and Actuators (FEAAM GmbH) as a research assistant on special rotating electric machines before he switched to volabo GmbH as a development engineer for electrical machines in 2016.

Prof. Dr.-Ing. Dieter Gerling (Institute for Electrical Drives – Universitaet der Bundeswehr Muenchen – Werner-Heisenberg-Weg 39, 85579 Neubiberg, Germany – Email: dieter.gerling@unibw.de - url: www.unibw.de/EAA) Born in 1961, Prof. Gerling got his diploma and Ph.D. degrees in Electrical Engineering from the Technical University of Aachen, Germany in 1986 and 1992, respectively. From 1986 to 1999 he was with Philips Research Laboratories in Aachen, Germany as Research Scientist and later as Senior Scientist. In 1999 Dr. Gerling joined Robert Bosch GmbH in Bühl, Germany as Director. Since 2001 he is Full Professor and Head of the Institute of Electrical Drives at the University of Federal Defense Munich, Germany.